

# Effect of CeO<sub>2</sub> on the thermoelectric properties of WO<sub>3</sub>-based ceramics

Haiqing Wang<sup>a,\*</sup>, Zhongqiu Hua<sup>b</sup>, Shujie Peng<sup>a</sup>, Xiang Dong<sup>b</sup>, Liang Dong<sup>b</sup>, Yu Wang<sup>b</sup>

<sup>a</sup> School of Material Science and Engineering, Southwest Jiaotong University, Chengdu, Sichuan 610031, China

<sup>b</sup> School of Electrical Engineering, Southwest Jiaotong University, Chengdu, Sichuan 610031, China

Received 1 June 2011; received in revised form 15 August 2011; accepted 22 August 2011

Available online 31 August 2011

## Abstract

The thermoelectric properties of tungsten trioxide (WO<sub>3</sub>) ceramics doped with cerium dioxide (CeO<sub>2</sub>) were investigated. The results demonstrated that the addition of CeO<sub>2</sub> to WO<sub>3</sub> could promote the grain growth and the densification. The magnitude of the electrical conductivity ( $\sigma$ ) and the absolute value of the Seebeck coefficient ( $|S|$ ) depended strongly on the CeO<sub>2</sub> content. The sample doped with 2.0 mol% CeO<sub>2</sub> yielded higher  $\sigma$  and  $|S|$ , resulting in a significant increase in the power factor ( $\sigma S^2$ ). In addition, the power factor value of all samples increased abruptly at high temperatures, which revealed that WO<sub>3</sub>-based ceramics could have greater thermoelectric properties at high temperatures.

© 2011 Elsevier Ltd and Techna Group S.r.l. All rights reserved.

**Keywords:** C. Electrical conductivity; Seebeck coefficient; WO<sub>3</sub> ceramics; Power factor

## 1. Introduction

Since Seebeck [1] observed the thermoelectric effect for the first time in 1823, PbTe [2,3] and SiGe alloys [4,5] have been extensively studied as materials for high temperature thermoelectric power generation. However, the practical applications of these materials have been limited, because these materials are easily decomposed or oxidized at high temperatures. To overcome the foregoing problems, metal oxides have been exploited as candidates for applications in thermoelectric generation due to their great thermal and chemical stability at high temperatures [6–8].

The oxide thermoelectric materials have been investigated considerably from a discovery of some layered p-type cobalt oxides, which have a comparable figure of merit to the conventional materials [9]. In 1997, Japanese scientists [10] found that the porous Y<sub>2</sub>O<sub>3</sub> ceramic exhibited huge Seebeck coefficient values up to  $-50$  mV/K at 900–1000 K in vacuum. Since then, great attention has been focused on the metal oxides, and some oxides such as ZnO, LaCoO<sub>3</sub>, NaCo<sub>2</sub>O<sub>4</sub> and SrTiO<sub>3</sub> have been widely studied [6–9,11]. Because the physical and chemical properties of WO<sub>3</sub> and SnO<sub>2</sub> ceramics as metal oxide semiconductors are similar to ZnO, the

applications of WO<sub>3</sub> in varistors and gas sensors are basically the same as ZnO [12–15]. Therefore, WO<sub>3</sub> ceramics could be utilized as thermoelectric materials. However, few studies on the thermoelectric properties of WO<sub>3</sub> have been reported. In the present study, the thermoelectric properties of WO<sub>3</sub>-based ceramics doped with CeO<sub>2</sub> were investigated for the first time.

## 2. Experimental procedure

In this work, analytical-grade raw materials of WO<sub>3</sub> (purity  $\geq 99.9\%$ ) and CeO<sub>2</sub> ( $\geq 99.99\%$ ) were used in compositions of  $(100 - x)$  mol% WO<sub>3</sub> +  $x$  mol% CeO<sub>2</sub>, where  $x = 0.0, 0.5, 2.0$  and  $4.0$ . After milled with agate balls and ethanol for 10 h, the powders were then granulated with binder and pressed at 100 MPa to form discs 10 mm in diameter and 3 mm in thickness. The discs with the same concentration were sintered at 1000 °C in air for 2 h. The heating rate was maintained at 100 °C/h.

The microstructure of samples was examined using scanning electron microscopy (FEI QUANTA200 with an energy dispersive spectrometer). As for the SEM and EDX analysis, samples were cleaned in acetone, mounted, and gold-coated to prevent charging. Average grain sizes of the CeO<sub>2</sub>-doped WO<sub>3</sub> ceramics have been estimated by the line-intersecting method, and the porosity of the specimens has been measured by the Archimedes principle. The crystalline phases of these sintered

\* Corresponding author. Tel.: +86 028 8760 1134; fax: +86 028 8760 0787.

E-mail address: [whq20054692@126.com](mailto:whq20054692@126.com) (H. Wang).

samples were identified by X-ray diffraction technologies (7602EA ALMELO) under the following experimental conditions:  $\lambda(\text{Cu K}\alpha) = 0.15406 \text{ nm}$ , 40 kV, 40 mA,  $20 \leq 2\theta \leq 60^\circ$ . The electrical conductivity from 323 K to 673 K was measured by means of a standard four-probe method using the KEITHLEY 2400. The thermoelectric power from 323 K to 673 K was calculated from the thermoelectric voltage collected with KEITHLEY 2400 and the temperature difference between the two ends of the sample.

### 3. Results and discussion

Fig. 1 shows the SEM micrographs of the sintered  $\text{WO}_3$  ceramics with different amount of  $\text{CeO}_2$ . It can be seen that the grain size and the densification of the  $\text{WO}_3$ -based ceramics become greater with the increasing  $\text{CeO}_2$  content. The rod-shaped structure can be evidently observed at the grain boundary regions as samples contain more than 0.5 mol%  $\text{CeO}_2$ . As shown in Fig. 2, the EDX spectra of the rod-shaped structure for  $\text{WO}_3$  ceramics doped with 2.0 mol%  $\text{CeO}_2$  indicates that the Ce-rich phase exists between  $\text{WO}_3$  grains. The grain size and the porosity of the samples are given in Table 1. Previous studies [13–15] suggested that the grain size of  $\text{WO}_3$ -based ceramics remained almost constant with an average grain size about  $10 \mu\text{m}$  and that the open porosity was about 14%. The grain size and the porosity in this research lie in the range  $7.1\text{--}11.7 \mu\text{m}$  and  $7.19\text{--}18.51\%$ , respectively. Moreover, the grain size of the doped samples is obviously larger than the undoped one. Therefore, the addition of  $\text{CeO}_2$  into  $\text{WO}_3$  ceramics can improve the mass transfer during sintering process, leading to the grain growth and the increasing densification.

The densification of the  $\text{SnO}_2\text{--CoO}$ ,  $\text{SnO}_2\text{--MnO}_2$  and  $\text{SnO}_2\text{--TiO}_2$  polycrystalline systems is attributed to the

increased concentration of oxygen vacancies in the grain boundary region [16,17]. The densifying mechanism of the  $\text{WO}_3\text{--CeO}_2$  ceramics may be similar to the one that occurs in the  $\text{SnO}_2$ -based ceramics, and the formation of oxygen vacancies could obey the following reactions:



Doping  $\text{WO}_3$  with  $\text{CeO}_2$  leads to the creation of additional oxygen vacancies that increase the flux of oxygen ions and promote  $\text{WO}_3$  grain growth and densification. However, there is a Ce-rich phase existing between  $\text{WO}_3$  grains in samples containing 2.0 and 4.0 mol%  $\text{CeO}_2$ , so the added  $\text{CeO}_2$  does not fully dissolve in the  $\text{WO}_3$  crystal lattice. As the content of  $\text{CeO}_2$  in  $\text{WO}_3$  is below its solubility limit in  $\text{WO}_3$ , the reaction that  $\text{CeO}_2$  dissolves in  $\text{WO}_3$  occurs. If the amount of  $\text{CeO}_2$  exceeds the solubility in  $\text{WO}_3$ , the extra  $\text{CeO}_2$  reacts with  $\text{WO}_3$  to form  $\text{Ce}_2\text{O}_3 \cdot 3\text{WO}_3$  [18], that is,  $\text{Ce}_2\text{W}_3\text{O}_{12}$ . The addition of  $\text{CeO}_2$  can promote the grain growth and the densification of the  $\text{WO}_3$ -based ceramics, while the second phase  $\text{Ce}_2\text{W}_3\text{O}_{12}$  lower the grain boundary mobility during sintering process and enable the pores to stay attached to the moving grain boundaries. Therefore, in spite of the slightly bigger grain size, the densification of the sample doped with 4.0 mol%  $\text{CeO}_2$  is worse than that of the one with 2.0 mol%  $\text{CeO}_2$ .

The XRD patterns given in Fig. 3 reveal that there is an obvious second phase in the doped samples when the content of  $\text{CeO}_2$  exceeds 0.5 mol%. The result is sharply different from the previous study [12]. Only monoclinic phase  $\text{WO}_3$  ( $\gamma\text{-WO}_3$ ) can be distinctly observed in the sample containing 0.5 mol%  $\text{CeO}_2$ , which is distinct from the co-existence of monoclinic and triclinic phases in undoped  $\text{WO}_3$  ceramics [13], implying that the form of the triclinic phase  $\text{WO}_3$  is effectively depressed by doping slightly  $\text{CeO}_2$ . Moreover, the rod-shaped inter-granular phase present in specimens doped with 2.0 and

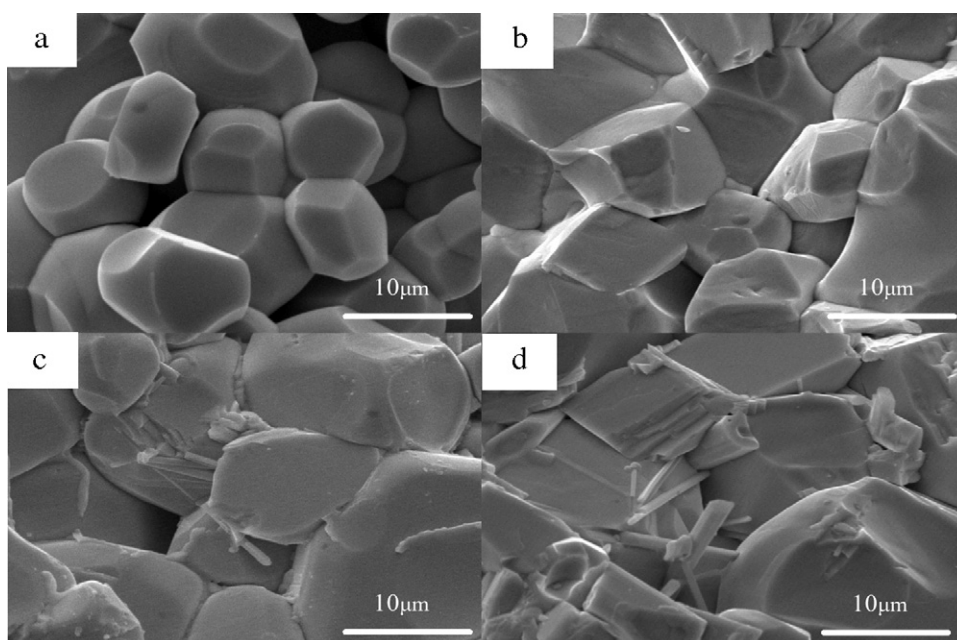


Fig. 1. SEM images of the samples  $(100 - x) \text{ mol\% } \text{WO}_3 + x \text{ mol\% } \text{CeO}_2$ : (a)  $x = 0.0$ ; (b)  $x = 0.5$ ; (c)  $x = 2.0$ ; and (d)  $x = 4.0$ .

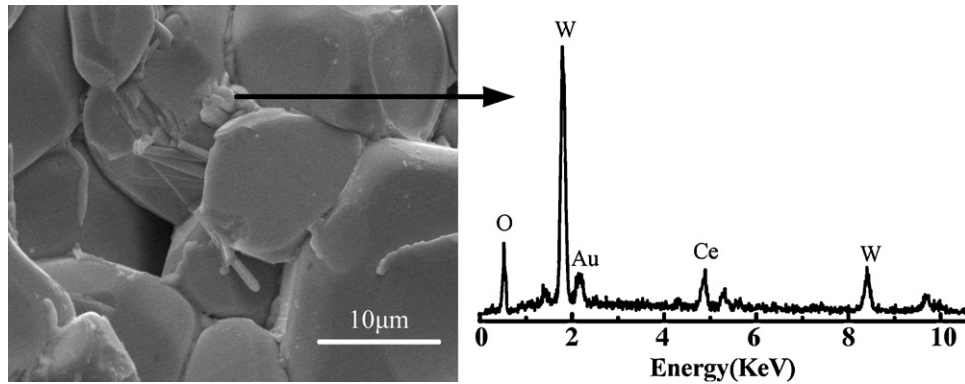


Fig. 2. EDX spectra of grain boundary regions for WO<sub>3</sub> ceramics doped with 2.0 mol% CeO<sub>2</sub> content.

4.0 mol% CeO<sub>2</sub> is identified as Ce<sub>2</sub>W<sub>3</sub>O<sub>12</sub> (JCPDS file card number 31-0340) through the XRD analysis.

The temperature dependence of the electrical conductivity ( $\sigma$ ) for samples is shown in Fig. 4(a). It can be observed that the curves of  $\log_{10} \sigma$  against  $1000/T$  exhibit approximately a linear characteristic overall, showing a semiconducting behavior which obeys the Arrhenius law:

$$\sigma(T) = \sigma_0 \exp\left(\frac{-E_a}{kT}\right) \quad (2)$$

where  $\sigma$  is the electrical conductivity,  $\sigma_0$  is a constant,  $k$  is the Boltzmann constant, and  $T$  is the absolute temperature. The activation energy of the samples has been evaluated and can be seen in Table 2. It can be noted that there are two activation energies one for low and the other for higher temperatures. This has been reported in Refs. [19,20], and the variation of the activation energy is due to the WO<sub>3</sub> phase transition at temperatures between 300 and 375 °C where  $1000/T$  is between 1.5 and 1.7 K<sup>-1</sup>. The result also demonstrates that the electrical conductivity of the doped WO<sub>3</sub> samples is lower than the pure one. The grain size and the porosity of the sample have notable effects on its thermoelectric properties. As the grain size is below 2 μm, the Seebeck coefficient sharply increases with the grain size decreasing, while the grain size is above 2 μm, the size effect of grain is not significant [21]. The grain size of all samples in this study is about 10 μm, and thus the grain size effect on the thermoelectric properties is not apparent. The additional scattering of phonons and electrons can happen at the pore sites or at the grain boundaries, so the porosity can degrade the electrical conductivity and the Seebeck coefficient [22]. The porosity of the doped samples is smaller than that of the undoped one, but the electrical conductivity of the doped ones is lower. This could be ascribed to the reduction of the electron

concentration by adding Ce<sup>4+</sup> for W<sup>6+</sup>, which can be explained by the same mechanism as adding TiO<sub>2</sub> into WO<sub>3</sub> [23] and doping ZnO with Sb<sub>2</sub>O<sub>3</sub> [24] and can have significant effects on the electrical conductivity. In the doped samples, the density and the grain size are greater with more CeO<sub>2</sub>, so the time between electron scattering events of charge carriers increases, and thus the electrical conductivity of the doped ones rises with the increasing content of CeO<sub>2</sub>.

Fig. 4(b) shows the Seebeck coefficients for all samples at different temperatures. The Seebeck coefficient values are all negative over the whole temperature range, indicating an n-type conduction. It is apparent that the absolute value of the Seebeck coefficient for the sample containing 2.0 mol% CeO<sub>2</sub> is larger than that of others. In general, the Seebeck coefficient decreases with increasing electrical conductivity [8,24]. Nevertheless, it can be seen in Fig. 4(b) that the absolute value of the Seebeck coefficient follows this rule except the specimen containing

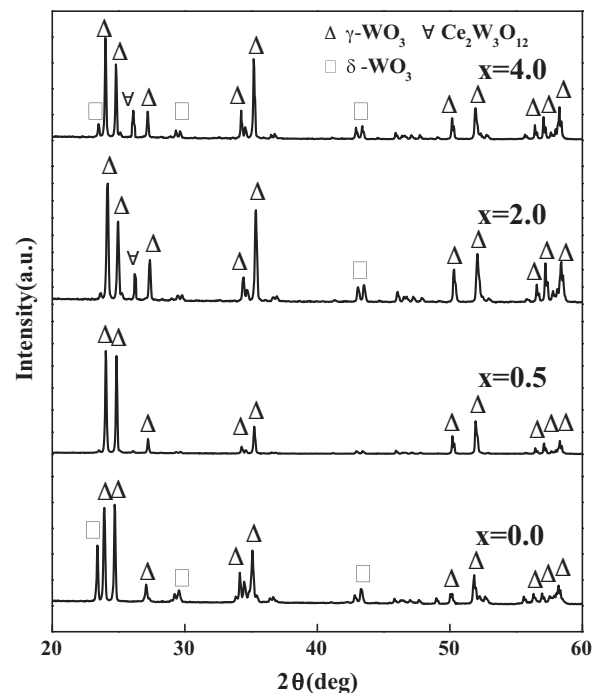


Fig. 3. XRD patterns of the (100 -  $x$ ) mol% WO<sub>3</sub> +  $x$  mol% CeO<sub>2</sub> samples.

Table 1  
Grain size and porosity of the samples with different CeO<sub>2</sub> contents.

CeO <sub>2</sub> (mol%)	Grain size (μm)	Porosity (%)
0.0	7.1	18.51
0.5	9.4	10.47
2.0	11.5	7.19
4.0	11.7	7.95

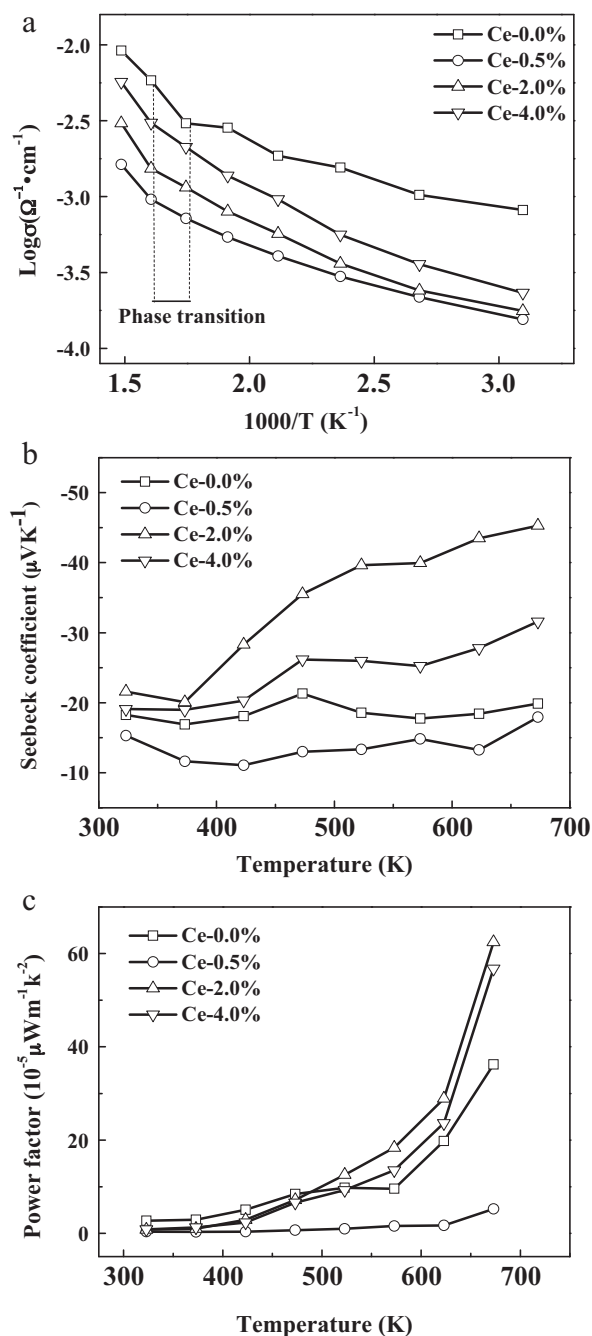


Fig. 4. Temperature dependence of (a) electrical conductivity, (b) Seebeck coefficient, and (c) power factor of the samples with different amount of CeO<sub>2</sub>.

0.5 mol% CeO<sub>2</sub>. Moreover, when the temperature is under 573 K, the Seebeck coefficient is almost constant for the undoped sample and the one with 0.5 mol% addition of CeO<sub>2</sub>. As the temperature is above 600 K, the Seebeck coefficient of them gradually goes up with the increasing temperature. According to the foregoing discussion, the grain size and the porosity of the sample have remarkable effects on its thermoelectric properties. The pure WO<sub>3</sub> ceramics is not densification and the porosity is tremendous, so the additional scattering of phonons and electrons occurs at the pore sites or at the grain boundaries, which degrades the Seebeck coefficient and makes it almost constant. For the sample with an addition of

Table 2

Activation energy of the samples with different amount of CeO<sub>2</sub> before and after the phase transition.

CeO <sub>2</sub> (mol%)	$E_a$ (eV) (before phase transition)	$E_a$ (eV) (after phase transition)
0.0	$0.063 \pm 0.003$	$0.330 \pm 0.005$
0.5	$0.108 \pm 0.003$	$0.386 \pm 0.005$
2.0	$0.158 \pm 0.003$	$0.502 \pm 0.005$
4.0	$0.187 \pm 0.003$	$0.451 \pm 0.005$

0.5 mol% CeO<sub>2</sub>, its Seebeck coefficient could be influenced by the following two factors. One is that the Ce ions dissolving in WO<sub>3</sub> block the migration of the carriers and thus slow down the mobility of the carriers even at high temperatures. The other is that the porosity of it is still large and the additional scattering of phonons and electrons occurs. Since the porosity of the specimens with 2.0 and 4.0 mol% CeO<sub>2</sub> is smaller, the Seebeck coefficient of them is better than that of others.

The thermoelectric power factor ( $\sigma S^2$ ) of all specimens, calculated from the data in Fig. 4(a) and (b), as a function of temperature is illustrated in Fig. 4(c). The power factor of WO<sub>3</sub>-based ceramics is improved by CeO<sub>2</sub> addition and increases with the temperature rising. The sample containing 2.0 mol% CeO<sub>2</sub> obtains the largest power factor with a value of  $6.25 \times 10^{-4} \mu\text{W m}^{-1} \text{K}^{-2}$  at 673 K. Although the Seebeck coefficient and the power factor of WO<sub>3</sub> are lower than that of ZnO [24], it is still attractive to research the thermoelectric properties of WO<sub>3</sub>, because it could be improved in some ways. Previous study [15] revealed that the quenched WO<sub>3</sub> ceramics exhibited a very low resistivity with a value of  $1.95 \Omega \text{ cm}$  at room temperature, that is to say, a very high conductivity. Moreover, it can be seen that the power factor of samples increases abruptly at the temperature above 600 K, implying a great performance at high temperatures.

#### 4. Conclusions

The thermoelectric properties of WO<sub>3</sub>-based ceramics have been investigated. The results demonstrate that doping CeO<sub>2</sub> can promote the grain growth and inhibit the porosity. The grain size and the porosity of samples have prominent effects on the thermoelectric characteristic. The Seebeck coefficient of the pure WO<sub>3</sub> ceramics is smaller than that of the ZnO-based ceramics, so it is important to densify the WO<sub>3</sub>-based samples to obtain a better thermoelectric performance. The thermoelectric properties of WO<sub>3</sub>-based ceramics at moderate temperatures are investigated for the first time, and thus the thermal diffusivity coefficients of samples have not measured in this work. However, the power factor of samples increases abruptly at the temperature above 600 K, indicating a better performance at high temperatures. The present results suggest that WO<sub>3</sub>-based ceramics could be a candidate for high temperature thermoelectric power generation.

#### Acknowledgment

This work was supported by the National Natural Science Foundation of China under Grant No. 50772092.

## References

- [1] T.J. Seebeck, Magnetic polarization of metals and minerals, Abh. K. Akd. Wiss. Berlin (1823) 265–373.
- [2] M.P. Singh, C.M. Bhandari, Non-monotonic thermoelectric behavior of lead telluride in quantum-well-like structures, Solid State Commun. 133 (2005) 29–34.
- [3] M. Ito, W.S. Seo, K. Koumoto, Thermoelectric properties of PbTe thin films prepared by gas evaporation method, J. Mater. Res. 14 (1999) 209–212.
- [4] D.M. Rowe, V.S. Shukla, The effect of phonon-grain boundary scattering on the lattice thermal conductivity and thermoelectric conversion efficiency of heavily doped fine-grained, hot-pressed silicon germanium alloy, J. Appl. Phys. 52 (1981) 7421–7426.
- [5] C.B. Vining, W. Laskow, J.O. Hanson, R.R. Van Der Beck, P.D. Gorsuch, Thermoelectric properties of pressure-sintered  $\text{Si}_{0.8}\text{Ge}_{0.2}$  thermoelectric alloys, J. Appl. Phys. 69 (1991) 4333–4340.
- [6] D. Bérardan, C. Byl, N. Dragoe, Influence of the preparation conditions on the thermoelectric properties of Al-doped ZnO, J. Am. Ceram. Soc. 93 (2010) 2352–2358.
- [7] F. Li, J.F. Li, Effect of Ni substitution on electrical and thermoelectric properties of  $\text{LaCoO}_3$  ceramics, Ceram. Int. 37 (2011) 105–110.
- [8] K. Park, K.U. Jang, H.C. Kwon, J.G. Kim, W.S. Cho, Influence of partial substitution of Cu for Co on the thermoelectric properties of  $\text{NaCo}_2\text{O}_4$ , J. Alloys Compd. 419 (2006) 213–219.
- [9] I. Terasaki, Y. Sasago, K. Uchinokura, Large thermoelectric power in  $\text{NaCo}_2\text{O}_4$  single crystals, Phys. Rev. B 56 (1997) R12685–R12687.
- [10] K. Koumoto, W.S. Seo, S. Ozawa, Huge thermopower of porous  $\text{Y}_2\text{O}_3$ , Appl. Phys. Lett. 71 (1997) 1475–1476.
- [11] Y.F. Wang, K.H. Lee, H. Ohta, K. Koumoto, Fabrication and thermoelectric properties of heavily rare-earth metal-doped  $\text{SrO}(\text{SrTiO}_3)_n$  ( $n = 1, 2$ ) ceramics, Ceram. Int. 34 (2008) 849–852.
- [12] X.S. Yang, Y. Wang, L. Dong, M. Chen, F. Zhang, L.Z. Qi, Effect of  $\text{CeO}_2$  on the microstructure and electrical properties of  $\text{WO}_3$  capacitor–varistor ceramics, Mater. Sci. Eng. B 110 (2004) 6–10.
- [13] Y. Wang, K.L. Yao, Z.L. Liu, Novel nonlinear current–voltage characteristics of sintered tungsten oxide, J. Mater. Sci. Lett. 20 (2001) 1741–1743.
- [14] Z. Hua, Y. Wang, H. Wang, L. Dong,  $\text{NO}_2$  sensing properties of  $\text{WO}_3$  varistor-type gas sensor, Sens. Actuators B 150 (2010) 588–593.
- [15] Z. Hua, L. Dong, H. Wang, S. Peng, Y. Wang, Varistor behavior study in undoped tungsten trioxide ceramic, Physica B 406 (2011) 2807–2810.
- [16] J.A. Cerri, E.R. Leite, D. Gouvêa, E. Longo, J.A. Varela, Effect of cobalt(II) oxide and manganese(IV) oxide on sintering of tin(IV) oxide, J. Am. Ceram. Soc. 79 (1996) 799–804.
- [17] P.R. Bueno, E.R. Leite, L.O.S. Bulhões, E. Longo, C.O. Paiva-Santos, Sintering and mass transport features of  $(\text{Sn,Ti})\text{O}_2$  polycrystalline ceramics, J. Eur. Ceram. Soc. 23 (2003) 887–896.
- [18] P.S. Anjana, T. Joseph, M.T. Sebastian, Low temperature sintering and microwave dielectric properties of  $\text{Ce}_2(\text{WO}_4)_3$  ceramics, Ceram. Int. 36 (2010) 1535–1540.
- [19] W. Sahle, M. Nyren, Electrical conductivity and high resolution electron microscopy studies of  $\text{WO}_{3-x}$  crystals with  $0 \leq x \leq 0.28$ , J. Solid State Chem. 48 (1983) 154–160.
- [20] Z. Pintér, Z. Sassi, S. Kornely, Ch. Pion, I.V. Perczel, K. Kovács, R. Bene, J.C. Bureau, F. Réti, Thermal behaviour of  $\text{WO}_3$  and  $\text{WO}_3/\text{TiO}_2$  materials, Thin Solid Films 391 (2001) 243–246.
- [21] H. Lee, D. Vashaee, D.Z. Wang, M.S. Dresselhaus, Z.F. Ren, G. Chen, Effects of nanoscale porosity on thermoelectric properties of SiGe, J. Appl. Phys. 107 (2010) 094308, 7 pp.
- [22] Y.W. Gao, Y.Z. He, L.L. Zhu, Impact of grain size on the Seebeck coefficient of bulk polycrystalline thermoelectric materials, Chin. Sci. Bull. 55 (2010) 16–21.
- [23] S. Komornicki, M. Radecka, P. Sobaś, Structural, electrical and optical properties of  $\text{TiO}_2\text{--WO}_3$  polycrystalline ceramics, Mater. Res. Bull. 39 (2004) 2007–2017.
- [24] K. Park, J.K. Seong, S. Nahm, Improvement of thermoelectric properties with the addition of Sb to ZnO, J. Alloys Compd. 455 (2008) 331–335.